

# Calibrated LCD/TFT stimulus presentation for visual psychophysics in fMRI<sup>☆</sup>

H. Strasburger<sup>a,\*</sup>, T. Wüstenberg<sup>b</sup>, L. Jäncke<sup>b</sup>

<sup>a</sup> Generation Research Program Bad Tölz, Human Studies Center, Ludwig-Maximilians-Universität München, Arzbacherstr. 12, D-83646 Bad Tölz, Germany

<sup>b</sup> Inst. f. Allgemeine Psychologie, Otto-von-Guericke-Universität, Magdeburg, Germany

Received 24 July 2002; received in revised form 15 August 2002; accepted 16 August 2002

## Abstract

Standard projection techniques using liquid crystal (LCD) or thin-film transistor (TFT) technology show drastic distortions in luminance and contrast characteristics across the screen and across grey levels. Common luminance measurement and calibration techniques are not applicable in the vicinity of MRI scanners. With the aid of a fibre optic, we measured screen luminances for the full space of screen position and image grey values and on that basis developed a compensation technique that involves both luminance homogenisation and position-dependent gamma correction. By the technique described, images displayed to a subject in functional MRI can be specified with high precision by a matrix of desired luminance values rather than by local grey value.

© 2001 Elsevier Science B.V. All rights reserved.

**Keywords:** Psychophysics; Stimulus presentation; Vision research; Thin-film transistor projector; Cathode ray tube; Gamma correction; Screen luminance; MRI

## 1. Introduction

Common techniques from visual psychophysics for presenting well-calibrated stimuli on cathode ray tube displays (CRT) are not directly usable in functional magnetic imaging studies due to the disruptive effect of the MRI's high magnetic field on electronic apparatus in direct vicinity. Early attempts have used fibre-optic displays to transmit a visual stimulus to the subject (Cornelissen et al., 1997) but in recent years a common presentation method is to directly project stimuli from an liquid crystal (LCD) projector, located outside the MRI cabin, onto a matte screen at the entrance to the

MRI tube that is viewed through a mirror mounted in front of the subject. It is well known that with a constant grey value in the image file, i.e. a blank image, the luminance on a standard CRT screen varies markedly with the position on the screen where the pixel is displayed (Bach et al., 1997 for a review), but it is less well known that these variations are even more drastic with LCD technology. We became aware of the problem when we found presumably lateralised activation in the primary visual cortex by stimulation with Gabor gratings, presented at 10° eccentricity on the left and right horizontal meridian, on a standard LCD set-up (Fig. 1). The lateralization turned out to be likely artefactual and effectively caused by the non-uniformity of the stimulus that was visible to the subject.

Non-uniformity of luminance across the screen with an image of constant grey value may be described by the variation of steepness of the transmission function that links (local) luminance to the (local) grey value, often

<sup>☆</sup> Patent pending

\* Corresponding author. Tel.: +49-171-4756-550; fax: +49-89-4899-7770

E-mail addresses: [strasburger@uni-muenchen.de](mailto:strasburger@uni-muenchen.de) (H. Strasburger), [torsten.wuestenberg@nat.uni-magdeburg.de](mailto:torsten.wuestenberg@nat.uni-magdeburg.de) (T. Wüstenberg).

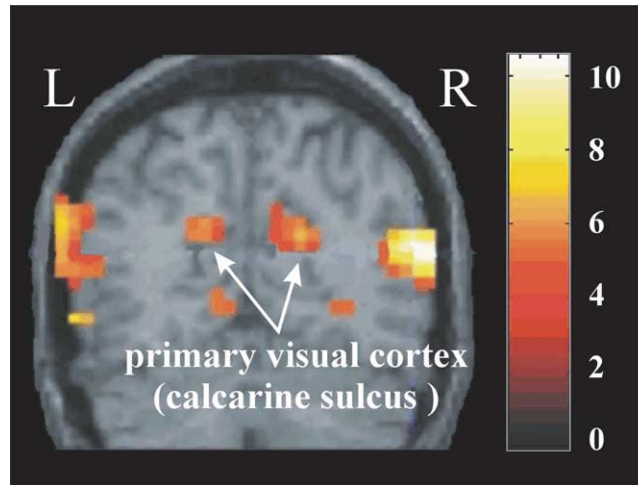


Fig. 1

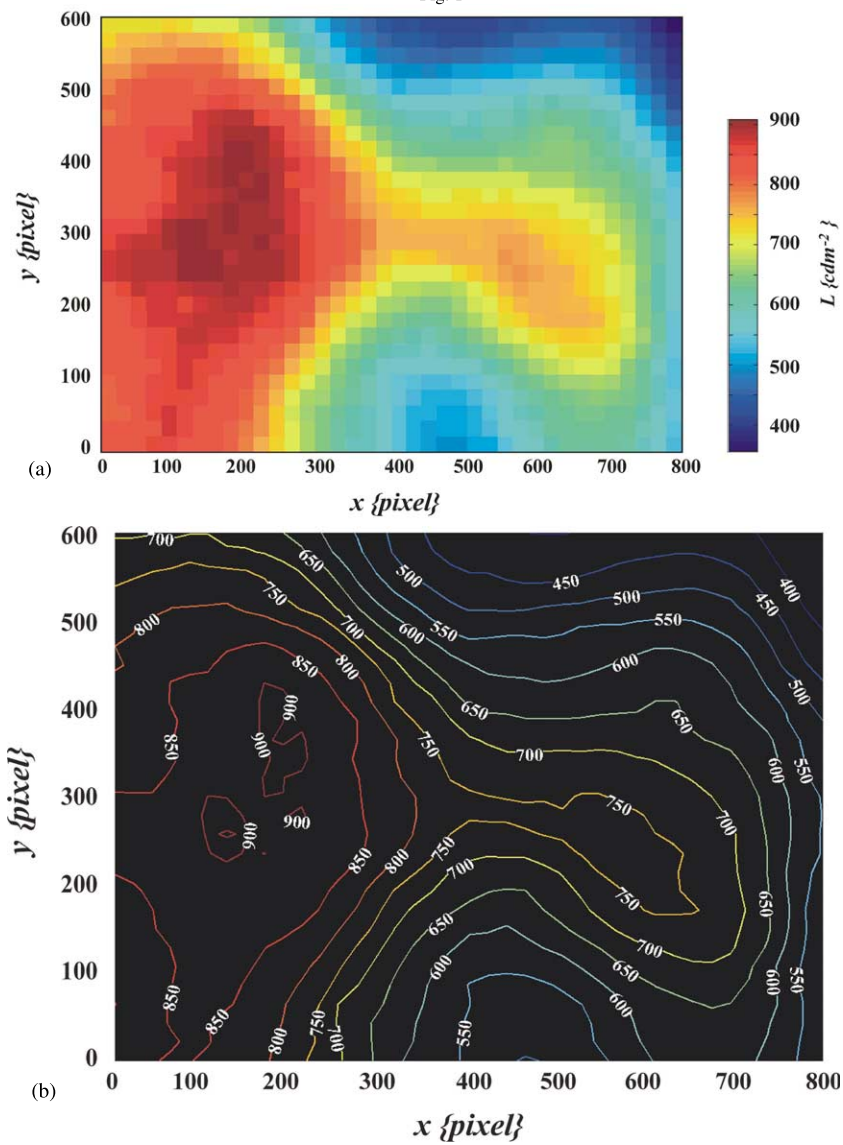


Fig. 2

Fig. 1. An example of a likely artifactual fMRI pattern caused by uncalibrated visual stimulation with a standard LCD/TFT projector system (Sharp).

Fig. 2. Uncalibrated luminance distribution on the matte screen visible to the subject, for constant grey value of 128. (a) Colour coded; (b) isoluminance contours.

known as the gamma function<sup>1</sup>. Fig. 2, more fully described below, shows the luminance distribution on our screen at a constant grey value of 128. Equally important however, the fact that the (non-uniform) gamma function is non-linear exaggerates these deviations from homogeneity in brighter-than-average parts of the screen, rendering, there, bright parts of the image over-proportionally brighter and the dark parts (less so) not dark enough (cf. Fig. 3; in other words: just adding a constant compensatory image will not suffice). We were thus motivated to derive a general model of the gamma function for all screen positions, that allows to predict the (actual) luminance for the full pixel parameter space, i.e. at any given screen position and any grey value. On that basis we developed a compensation technique that allows the experimenter to specify the target image as a matrix of desired luminance values rather than by local grey value.

## 2. Fibre optics for measuring screen luminance

Standard luminance meters cannot be used to measure screen luminance simply because they will not function in the scanner's vicinity. Knowing the precise luminance distribution visible to the subject is required for a successful calibration, however, so it is essential to measure luminance from within the scanner, i.e. with the stimulus set-up identical to that during any functional MRI recording. We therefore made a fibre-optic connection that allowed us to transmit the local luminance at the screen to a standard digital luminance meter located in the adjacent scanner control room. A single, plastic-shielded fibre of 10 m length, 1 mm diameter was used (Hirschmann Electronics type OKD 1000-B, core: 0.98 mm, total diameter 2.2 mm, attenuation at 660 nm: 220 dB/km), which at the 0.25-mm raster of our screen covered around 13 pixels. Onto the fibre cable's ends we mounted at right angle a  $1.5 \times 8.0$  cm<sup>2</sup> plastic plate by epoxy, such that at one end the cable could be steadily fastened to the luminance meter and at the other positioned at a defined position on the projection screen.

To determine the fibre optic's attenuation of light energy, 10 luminance measurements were taken at 25 of

the possible 256 grey values, both through the fibre optic and directly at the corresponding screen position. As to be expected, the attenuation is well described by a linear function. With the regression forced through zero and the attenuated signal treated as predictor variable, the (inverse) transfer function is

$$L = 73.3L_{\text{att}}, \quad (r^2 = 0.9962), \quad (1)$$

i.e. the attenuation factor is 73.3 or 18.65 dB (dB defined as 10 dB per log unit).

## 3. Luminance distribution on the matte screen

The projector in our system (Sharp, model XG-SV 1E) has three LCD panels in thin-film transistor (TFT) active matrix driver technology having  $832 \times 624$  pixels each, lit by a 370 W metal-halogenide bulb. The image is projected onto a matte screen ( $600 \times 300$  mm<sup>2</sup>, 5 mm thick, one-side matte sheet of polymethylmetacrylate, i.e. Plexiglas), mounted at the entrance of the scanner's tube and viewed by the subject through a mirror located close to the subject's eyes.

Using the fibre optic and a digital luminance meter (type Mavo Monitor, manufactured by Gossen-Metrawatt, range 199.9 cd/m<sup>2</sup>, resolution 0.1 cd/m<sup>2</sup>, error 2.5% of value) we measured screen luminance in a raster of  $40 \times 30$  screen locations, taking 5 readings at each of the 1200 locations. One experimenter lay in the scanner's tube, holding the fibre optic's adapter to the screen at the required position that was displayed to him by a computer generated cross hair. The other took the readings on the luminance meter in the adjacent scanner control room. For each reading, the fibre-optic was set to the required position anew, to provide independent measurements. Measurements were performed on 2 days; at the beginning of a session the projector was left to warm up for 10 min. Fig. 2 shows the resulting luminance distribution on the screen, after correction through Eq. (1).

At the bright portions of the screen in the middle left ( $x = 140$ ,  $y = 240$ ), luminance is by a factor of three higher than at the darkest part in the upper right ( $x = 780$ ,  $y = 540$ ).

## 4. The gamma curve at characteristic screen positions

A full description of the display system's (static) transfer characteristic requires the specification of luminance as a function of grey value and pixel position, of which the luminance distribution shown in Fig. 2 represents a cross-section at constant mean grey value. To describe the dependency of luminance on grey value, five, in terms of their luminance representative positions on the screen ( $x_i, y_i$ ) were chosen from Fig. 2—at

<sup>1</sup> The term gamma function strictly applies to CRT displays only, where the transfer function mapping the analog voltage to screen luminance is an exponential, with a non-integer exponent between 2 and 3, traditionally denoted by the Greek letter gamma (Bach et al., 1997). The TFT transfer function is also non-linear, but is best described by a second-order polynomial, as will be seen below. The (somewhat colloquial) use of the term gamma function or gamma curve has become more widely spread in the technical literature so we will use it here as a readily understood short cut. The term is, by the way, unrelated to the gamma function in mathematics, by Euler, Gauß and others, the latter a generalization of the faculty function.

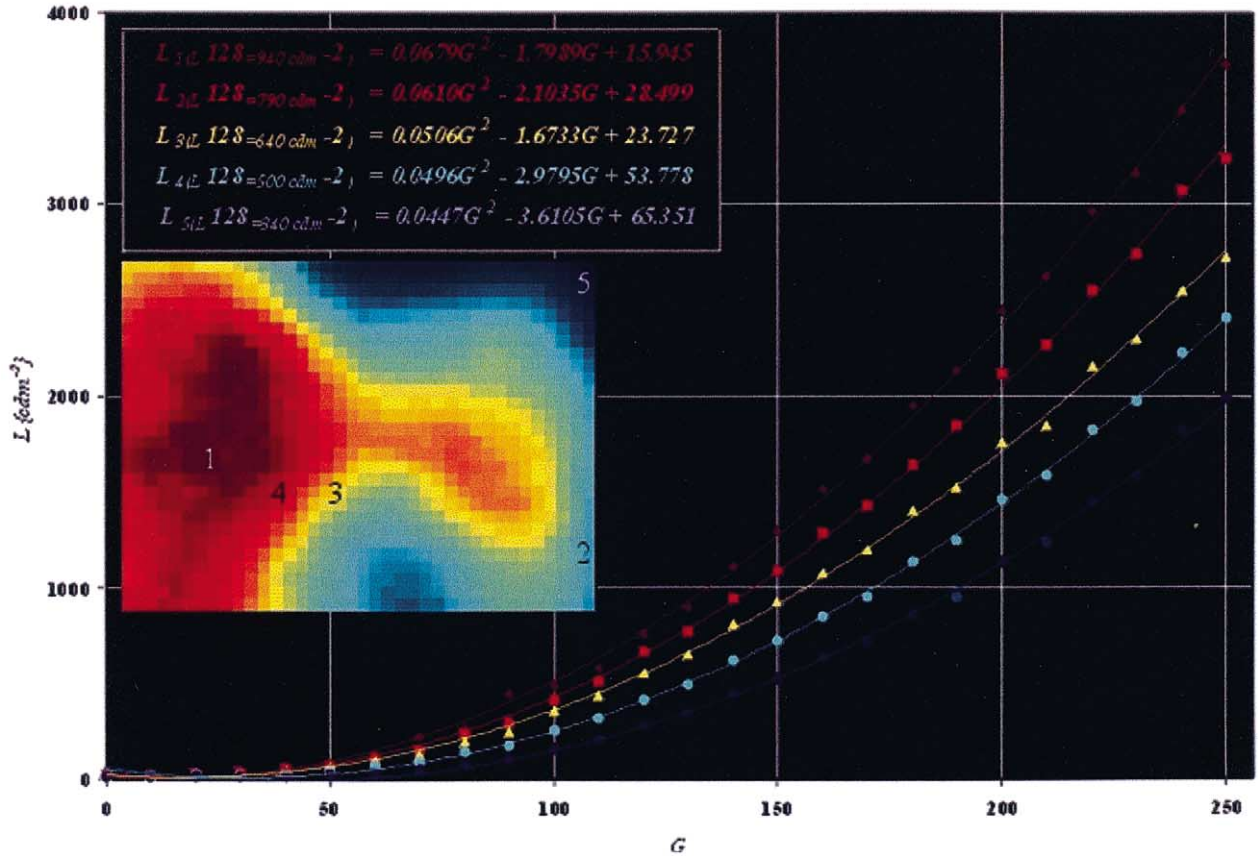


Fig. 3

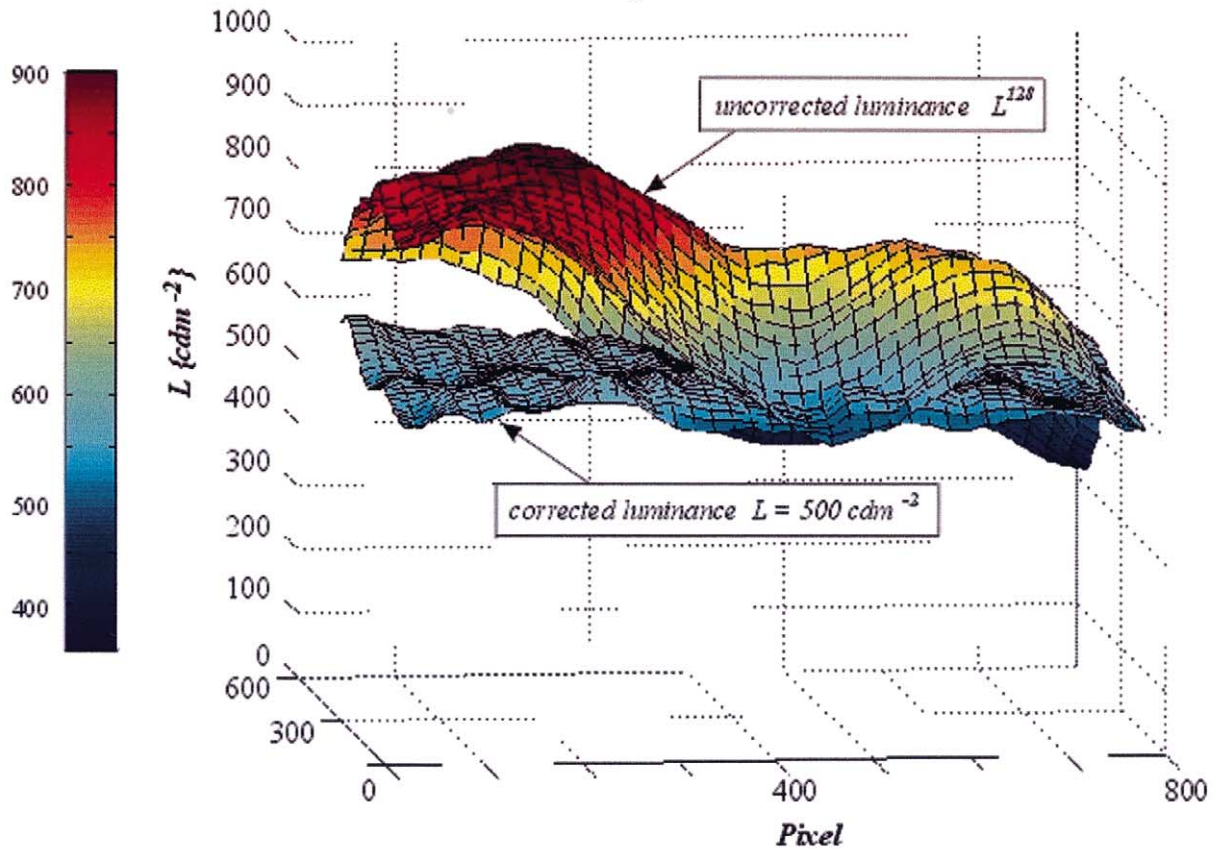


Fig. 5

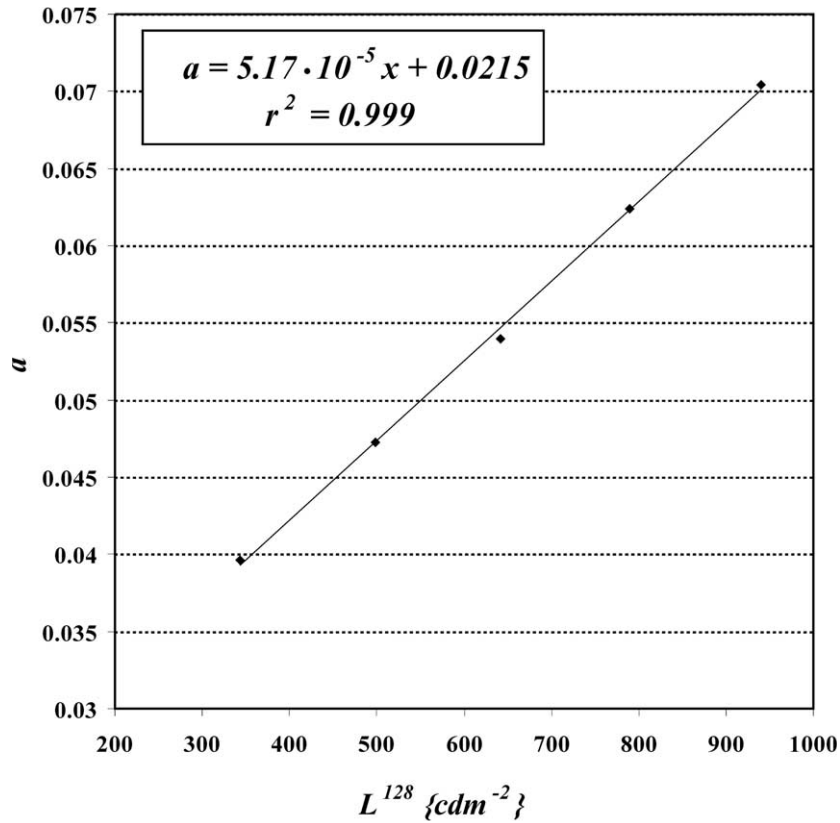


Fig. 4. Interpolation of the second-order term ( $a$ ) to arrive at a unified model for the gamma curve. (Note the equidistant choice of  $L^{128}$  values).

Table 1  
Regression coefficients of the gamma curve at the five screen positions

Location #	1	2	3	4	5	Mean
$X$	780	780	360	260	140	–
$Y$	540	100	160	160	240	–
$L^{128}$ (cd/m <sup>2</sup> )	340	500	640	790	940	–
$a$	0.0447	0.0496	0.0506	0.0610	0.0679	–
$b$	–3.6105	–2.9795	–1.6733	–2.1035	–1.7989	–2.43314
$c$	65.351	53.778	23.727	28.499	15.945	37.46
$r^2$	0.9991	0.9992	0.9991	0.9994	0.9986	0.9991

$x,y$ : pixel coordinate;  $L^{128}$ : luminance for grey value 128 in cd/m<sup>2</sup>;  $a, b, c$ : regression coefficients in Eq. (2);  $r^2$ : coefficient of determination.

maximum and minimum luminance, and at three roughly equally spaced luminance values in between (cf. Fig. 4 for the spacing)—and the full gamma curve was measured at these positions.

At each position, 10 measurements were taken at 25 equally spaced grey values, i.e. a total of  $5 \times 10 \times 25$  readings. The results are shown in Fig. 3. To each of the five sets of data, a second-order polynomial was fit by regression

$$L = a_{(x,y)}g^2 + b_{(x,y)}g + c_{(x,y)} \quad (2)$$

with  $g$ : grey value in the image file (all three colour values equal to  $g$ );  $(x,y)$ : screen position, and  $a, b$ , and  $c$ : position-dependent regression coefficients. The regression coefficients are summarized in Table 1. As can be seen from the coefficients of determination  $r^2$  (also given in the table), less than 1% of the variance remains unaccounted for.

Fig. 3. Gamma curve at five representative screen positions. The positions are indicated in the inset and in Table 1.

Fig. 5. Efficiency of the compensation. Top and bottom surface show the uncalibrated luminance distribution at grey value 128, and the calibrated distribution at 500 cd/m<sup>2</sup>, respectively.

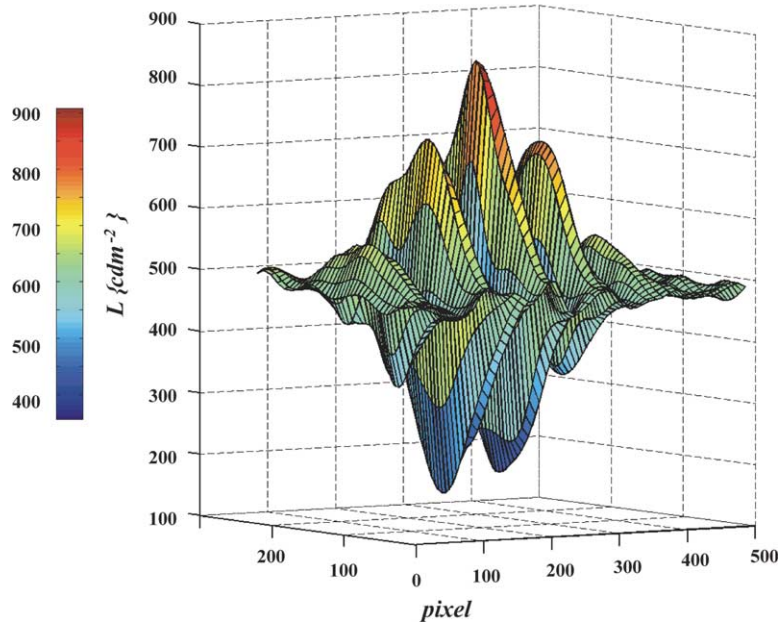


Fig. 6

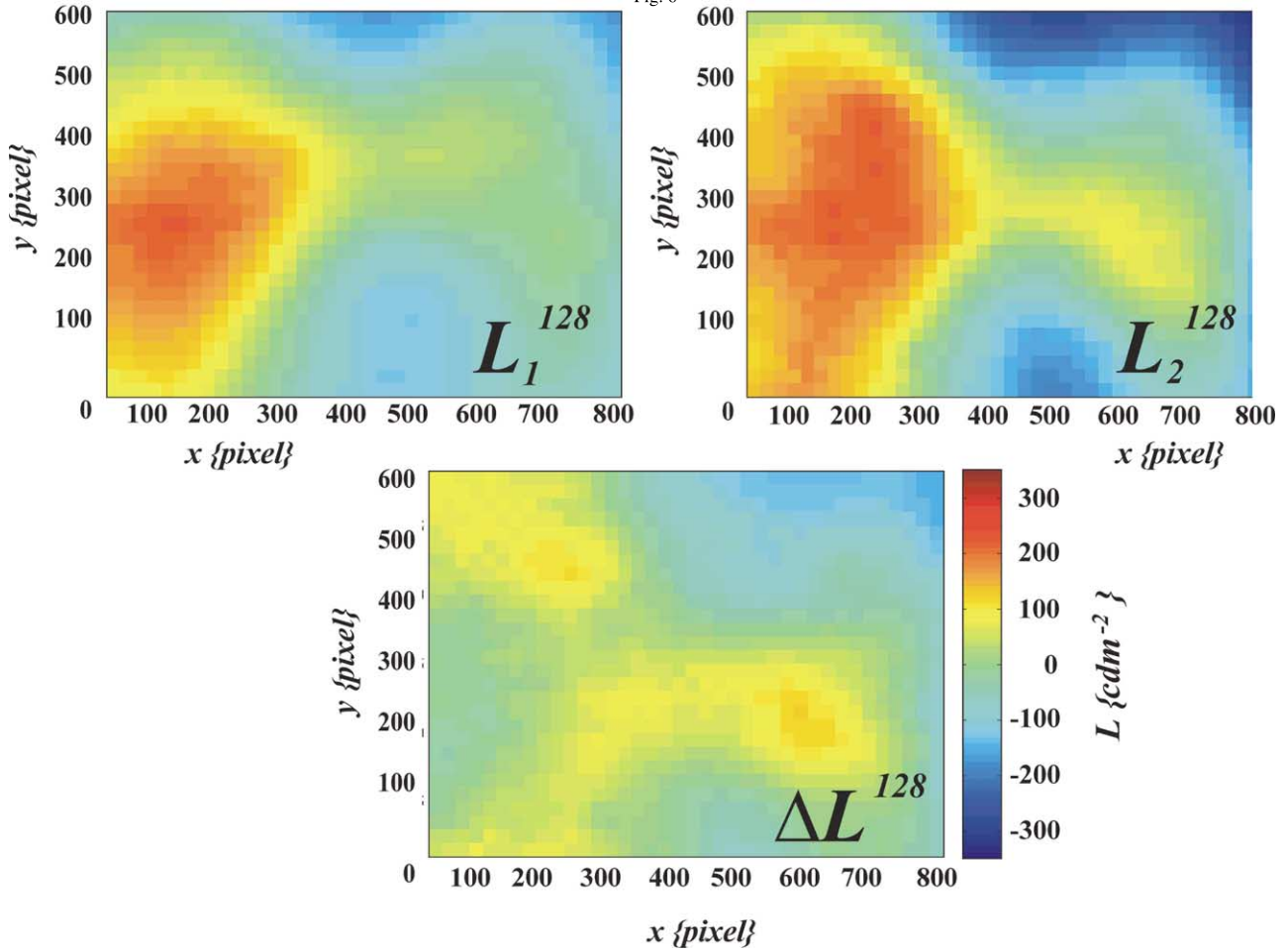


Fig. 7

Fig. 6. Measured luminance profile of a Gabor grating, with the luminance calibration in place. The Gabor grating luminance was sampled at  $25 \times 20$  screen positions with our fibre optic system.

Fig. 7. Long-term stability of the projector's luminance distribution. Figure part (a) and (b) show the uncalibrated luminance distribution on the matte screen  $1\frac{1}{2}$  years ago and today, respectively. There were one maintenance return to the manufacturer and one bulb replacement (which involves removing the bulb bearing cage) in between. (c) shows the pixelwise difference of the two distributions after equalizing to same mean luminance.

Table 2  
Second-order coefficients  $a$  and coefficients of determination,  $r^2$

Location #	1	2	3	4	5
$a$	0.03965	0.04729	0.05397	0.06238	0.07045
$r^2$	0.99635	0.99914	0.99858	0.9919	0.9989

## 5. The general gamma function

From the five gamma curves (considered representative of the population of curves), the task was to derive an approximation to the general function  $F((x,y), g)$ . Inspection of the set of regression coefficients in Table 1 shows that the linear term's coefficient  $b$  and the constant  $c$  vary considerably between the five. However, since the second-order term is expected to have the largest contribution to the overall range of luminance values predicted (0–2500 cd/m<sup>2</sup>) and to economize on the number of free parameters in the general model, we repeated the fits shown in Fig. 2 with both  $b$  and  $c$  forced, in the regression, to their respective arithmetic means (Table 1, last column):

$$L = a_{(x,y)}g^2 + bg + c; \quad (3)$$

$L$  is luminance in cd/m<sup>2</sup>,  $g$  is grey value (between 0 and 255), and  $a_{(x,y)}$  is free to vary. The resulting second-order coefficients and coefficients of determination are shown in Table 2. As can be seen from the  $r^2$ , the fits are about equally good as before, such that there is, indeed, little loss in assuming both  $b$  and  $c$  as constant.

We now need to establish a relation between the second-order term and the characteristics of a screen location. Screen position in itself is not relevant, and for describing a location's characteristic we have chosen the (empirical) luminance at that position at mean grey value, 128, denoted by  $L^{128}(x,y) = L^{128}$ . The variation of coefficient  $a$  was then described by regression onto  $L^{128}$ :

$$a(x,y) = pL_{128} + q, \quad (4)$$

where  $p$  and  $q$  are free parameters. The coefficient was remarkably well predicted by the linear Eq. (4) (Fig. 4); the resulting coefficients were  $p = 5.168 \times 10^{-5}$  and  $q = 0.0215$ .

The full model of the luminance transfer function is given by Eqs. (3) and (4), with the descriptive parameters  $b$ ,  $c$ ,  $p$ , and  $q$ .

With these parameters filled in for our set-up, as an example, the equations are

$$L = a(x,y)g^2 - 2.433g + 37.46, \quad (3a)$$

$$a(x,y) = 5.168 \times 10^{-5}L^{128} + 0.0215 \quad (4a)$$

Together with the matrix of luminance values at mean grey level,  $L^{128}(x,y)$ , these equations predict luminance at any grey value and screen position.

## 6. The corrected image

To arrive at desired grey values for a specified luminance  $L$ , Eq. (3) can be inverted to obtain  $g(L)$

$$g = -b/2a + \sqrt{[(b/2a)^2 + (L - c)/a]}, \quad (5)$$

with  $a = a_{(x,y)}$  being the second-order coefficient calculated from Eq. (4). For our set-up this becomes

$$g = 1.217/a + \sqrt{[(1.217/a)^2 + (L - 37.46)/a]}, \quad (5a)$$

Calculating the corrected images is then straightforward:

- 1) Calculate, from Eq. (4), the matrix of coefficients  $a(x_i,y_i)$  at the  $40 \times 30$  sample positions where  $L^{128}$  was measured;
- 2) by linear interpolation, calculate the full ( $832 \times 624$ ) matrix  $a_{(x,y)}$  at all pixel positions;
- 3) for the desired luminance  $L = L(x,y)$  at any pixel, obtain the required grey value  $g$  from Eq. (5).

Fig. 5 shows a comparison of the luminance distributions, specified as having constant luminance, before and after correction. Note that the 'wrinkled towel' at  $L^{128}$  (top surface) turns into a reasonably flat surface.

## 7. Dithering the corrected image

Changing any image along sharply defined raster lines leads to highly visible contours in otherwise homogeneous image regions. With the luminance correction in place, dithering of the corrected image is thus required. We chose the simplest version, Floyd-Steinberg error diffusion, in which at each pixel a random number from the interval  $[-1, 1]$  is added before rounding to the next integer. This is step (4) and the last step in determining the desired grey values.

For illustration of the efficiency of the procedure, Fig. 6 shows the (actual) luminance profile of a Gabor grating, sampled at  $25 \times 20$  screen positions with our fibre optic.

## 8. Practical considerations

Calibrating a monitor by the described technique is an investment: the 1800 measurements (1200 + 600) took us around 6 h. Will the work be lost when a change of the bulb is required? The luminance distributions shown in Fig. 2 are in fact from a second, current set of measurements. One and a half years earlier, we had taken the same measurements (1200 readings, around 4 h); in the meantime the monitor was once at the manufacturer for maintenance reasons and there was

one bulb replacement which involves removing of the bulb bearing cage and can be expected to slightly change the bulb's position in the optical arrangement. Fig. 7 shows the luminance distributions, i.e. the  $L^{128}$  matrix, at the two points in time. Interestingly, the basic pattern is not changed, with a bright region on the left that extends into the right. The change seems mostly a certain spatial distortion, possibly stemming from a slightly changed position of the bulb in the diffusion chamber. The changes are large enough, however, that they make a re-calibration worthwhile.

Even though, through age and bulb changes, the spatial  $L^{128}$  luminance distribution and mean image luminance were changed, the form of the gamma curve was little changed, in both cases being a second-order parabola dominated by the second-order term, the latter being linearly dependent on mean-grey-value luminance. The Eq. (3) and Eq. (4) for the old set-up were

$$L = a_{(x,y)}g^2 - 1.16g + 14.3, \quad (3b)$$

$$a_{(x,y)} = 5.59 \times 10^{-5}L^{128} + 0.00929 \quad (4b)$$

We can thus assume that the transparency characteristics of the LCD (responsible for the gamma curves) have not changed much over time and that the changes are brought about by a slightly changed optical arrangement and efficiency of the bulb. Such an assumption should simplify repeated calibration.

With the compensation technique in place, its practical application is straightforward. Images can be standard pixel graphics files (pcx, gif, etc.) from graphics programs or generated by graphic algorithms (e.g. in MatLab). The MatLab script calculates a corrected image file that is then used instead of the original in the stimulus presentation routine. Black/white videos can be processed by image-wise application of the MatLab script.

How significant is the use of a well-calibrated visual stimulation system in the context of fMRI research? The human visual system has a remarkable capability of compensating broad luminance variations by its insensitivity to low spatial frequencies and so the field non-homogeneities might seem less important than the

numbers suggest. Since the overall field size is quite small compared to the full visual field, however, these variations occur in close neighbourhood and local adaptation will play less of a role. The fact that the inhomogeneities are well visible implies that they are processed in cortical visual areas. Furthermore, since the gamma function also varies between screen positions, stimulus pattern contrast will vary across the field, and we know that the amplitude of the BOLD response depends on pattern contrast (Boynton et al., 1999). Scepticism is in particular called for when, with standard stimulation systems, subtle fMRI activations differences between hemispheres in primary visual areas are interpreted. Certainly, in neuro-ophthalmic diagnostics, much higher standards are observed, with background luminance in a standard perimeter being held constant within narrow limits. By the relatively straightforward compensation technique described here, luminance visible to the subject can be specified with good accuracy in the full (monochrome) space/luminance domain spanned by a standard 8-bit graphics system.

## Acknowledgements

The work was supported by DFG grant JA 737/5-2 to L. Jäncke and STR 354/3-1 to H. Strasburger. Thanks go to Dorothe Poggel, Katrin Schulze, Tino Zähle, Ulrike Bunzenthal and Iris Müller for help with the lengthy measurements.

## References

- Bach M, Meigen T, Strasburger H. Raster-scan cathode ray tubes for vision research—limits of resolution in space, time and intensity, and some solutions. *Spatial Vision* 1997;10:403–14.
- Boynton G, Demb J, Glover G, Heeger D. Neuronal basis of contrast discrimination. *Vision Research* 1999;39:257–69.
- Cornelissen F, Pelli DG, Farell B, Huckins SC, Szeverenyi NM. A binocular fiberscope for presenting visual stimuli during fMRI. *Spatial Vision* 1997;11:75–81.